

Synergy between ground and space based gravitational wave detectors for estimation of binary coalescence parameters

Remya Nair¹, Sanjay Jhingan¹, and Takahiro Tanaka^{2,3}

¹*Centre for Theoretical Physics, Jamia Millia Islamia, New Delhi -25, India*

²*Yukawa Institute for Theoretical Physics, Kyoto University, 606-8502, Kyoto, Japan and*

³*Department of Physics, Kyoto University, 606-8502, Kyoto, Japan*

We study the advantage of the co-existence of future ground and space based gravitational wave detectors, in estimating the parameters of a binary coalescence. Using the post-Newtonian waveform for the inspiral of non-spinning neutron star-black hole pairs in circular orbits, we study how the estimates for chirp mass, symmetric mass ratio, and time and phase at coalescence are improved by combining the data from different space-ground detector pairs. Since the gravitational waves produced by binary coalescence also provide a suitable domain where we can study strong field gravity, we also study the deviations from general relativity using the parameterized post-Einsteinian framework. As an example, focusing on the Einstein telescope and DECIGO pair, we demonstrate that there exists a sweet spot range of sensitivity in the pre-DECIGO phase where the best enhancement due to the synergy effect can be obtained for the estimates of the post-Newtonian waveform parameters as well as the modification parameters to general relativity.

PACS numbers: 04.30.-w, 04.50.Kd, 04.30.Db, 04.80.Nn, 95.55.Ym

I. INTRODUCTION

General relativity (GR) has enjoyed a very successful run as a theory describing the classical Universe by passing all the tests available so far [1]. Yet two of the unique predictions of GR, the black holes (BHs) and gravitational waves (GWs), are waiting for direct confirmation. There is an ever increasing indirect evidence of stellar mass BHs as well as super massive BHs at the center of each galaxy [2]. Similarly, the Universe is immersed in a GW background, analogous to the cosmic microwave background, but we still have no glimpse of it. Thanks to several decades of research developing detectors with ever increasing sensitivity, we are likely to be very close to detecting GWs and to open a new era in astronomy. It will not be an overstatement to say that if the 20th century belonged to astronomy with electromagnetic waves, the 21st century would definitely belong to astronomy with GWs [3, 4]. The detection of GWs would not only be a triumph of GR as the theory describing our classical world, but it would also give us a unique opportunity to detect BHs by directly mapping their spacetime.

GR has been subjected to a plethora of experimental tests, but mostly the explored regimes are those in which the gravitational field is weak and particle velocities are small relative to the speed of light [1]. Thus, one of the most promising outcomes of GW astronomy would be the possibility of testing the validity of GR in the dynamical strong field regime [5]. The prospect of discovering that GR may need some modification in the strong field regime has also motivated the development of several alternative theories of gravity. GW signals will provide a testing ground for these theories and a wide range of tests of GR have already been proposed. Tests that use GWs coming from compact binary coalescence include those proposed in [6–12]. The coalescing binaries composed of neutron stars (NS) and BHs are amongst the most likely sources for GW signals to be observed by ground-based interferometric detectors. When observed, these GW signals will probe the strong field regime of gravity and allow the implementation of these tests of GR.

The post-Newtonian formalism (PN) has been used to model the inspiral part of the binary evolution within GR. In the PN formalism physical quantities of interest such as the conserved energy, flux etc. are found as expansions in the small parameter (v/c) , where v is the characteristic speed of the binary system and c is the speed of light [13]. In standard convention $O((v/c)^n)$ corrections counting from the leading order are referred to as a $(n/2)$ PN order term. The expansion of the GW waveform is currently known up to 3.5PN, and the binary motion is known up to 4PN order [13]. Inspiring binaries are suitable for studying the strong field regime. The orbital velocities in these systems can go as high as $0.5c$, and therefore higher order PN corrections are relevant. The standard data analysis techniques used for the detection and analysis of GW signals depend on the availability of accurate templates to identify weak signals buried in the noise. However, in order to carry out the tests of GR, it is impractical to make accurate templates for all possible alternative theories of GR. A more feasible way of carrying such tests is to adopt general non-GR templates to model the signals. Arun et al., proposed such templates in which the expansion coefficients of the phase in the Fourier transform of the GW waveform (see equation (3) ahead) are treated as fitting parameters [9]. In GR each coefficient is specified by the masses and spins of the constituting compact objects of the binary. In principle, this relation can be completely different in some alternative theory and may even involve other parameters.

Yunes and Pretorius developed the parameterized post-Einsteinian (ppE) framework, which allows for characterizing a wider range of deviations to the amplitude and phase of the waveform [10]. Similar to the parameterized post-Newtonian framework they introduced ppE parameters, but instead of parametrizing the metric tensor, they parametrize the GW response function using a generic template family (see section II B ahead). This family can accommodate the inspiral phase of most of the known alternative theories with appropriate choices of the parameters. Cornish et al. applied the ppE approach to simulated data to determine the level at which departures from GR can be detected, and also analysed the bias introduced in the extraction of the model parameters due to the assumption of the wrong theory [11].

In this work we study the synergy between the ground and space based GW detectors in estimating the parameters of the inspiraling binaries, to see whether there is any gain in combining measurements from two detectors. For this we use the ppE framework developed by Yunes and Pretorius [10]. We consider two future space based detectors (DECIGO and eLISA) and two future ground based detectors (Advanced LIGO and ET). As representative test cases we consider two binary systems, a $1.4 M_\odot + 10 M_\odot$ binary and a $1.4 M_\odot + 100 M_\odot$ binary, where M_\odot is the solar mass. Within the PN framework, we study the synergy effect in detail for the chirp mass, the symmetric mass ratio and the time and phase at coalescence, and within the ppE framework we study the synergy effect on the estimation of the ppE parameter characterizing deviation from GR. The plan of the paper is as follows: in the next section we briefly describe the waveforms used in this analysis (II A, II B), the noise curves for the different detectors (II C), and the methodology for error estimation (II D). We summarise our results in section III.

II. METHODOLOGY

A. PN formalism

We use the PN expression for the Fourier transform $H(f)$, of the GW signal coming from the inspiral of binary compact objects in a circular orbit (under the stationary phase approximation) [14]. Moreover, the *restricted PN waveforms* are used which keep the higher terms in phase but only take the leading terms for the amplitude [15]. This is because in the matched filtering analysis used for the parameter estimation of binaries the correlation of two waveforms is more sensitive to deviation in phase than the amplitude. This is not true for binaries with misaligned spins, where the amplitude modulation on precession time scale is also important to determine the spin parameters [16]. As we consider non-spinning binaries for simplicity, this modulation is beyond the scope of this paper.

Hence we consider only the leading order term in the amplitude, while the phase terms are taken up to 3.5PN order (note that terms with exponent $k = n$ are $(n/2)$ PN order terms). Namely, we adopt the waveform

$$H(f) = \mathcal{A} f^{-7/6} \exp(i\psi(f) + i\pi/4), \quad (1)$$

where the Fourier amplitude \mathcal{A} is given by

$$\mathcal{A} = \frac{\mathcal{C}}{D\pi^{2/3}} \sqrt{\frac{5\nu}{24}} M^{5/6}, \quad (2)$$

and the phase $\psi(f)$ is given by

$$\psi(f) = 2\pi f t_c + \phi_c + \frac{3}{128\nu} \sum_{k=0}^7 \alpha_k (\pi M f)^{(k-5)/3}. \quad (3)$$

Here \mathcal{C} is an $O(1)$ dimensionless geometric factor that depends on the relative orientation of the binary and the detector (average over all orientations $\bar{\mathcal{C}} = 2/5$), ν is the symmetric mass ratio, M is the total mass of the binary, D is the luminosity distance and t_c and ϕ_c are the time and phase at coalescence, respectively. For the purpose of this paper, the explicit expression for \mathcal{C} is not necessary as we also neglect the effects of the orbital motion of the space antenna. The expressions for the amplitude and the phase are often also expressed in terms of the chirp mass $\mathcal{M} = \nu^{3/5} M$ as

$$\mathcal{A} = \frac{\mathcal{C}}{D\pi^{2/3}} \sqrt{\frac{5}{24}} \mathcal{M}^{5/6}, \quad (4)$$

and

$$\psi(f) = 2\pi f t_c + \phi_c + \frac{3}{128\nu} \sum_{k=0}^7 \alpha_k \left(\frac{\pi \mathcal{M} f}{\nu^{3/5}} \right)^{(k-5)/3}. \quad (5)$$

The values of the coefficients in the PN expansion of the Fourier phase are as follows [14]:

$$\begin{aligned}
\alpha_0 &= 1, \quad \alpha_1 = 0, \quad \alpha_2 = \frac{3715}{756} + \frac{55}{9}\nu, \\
\alpha_3 &= -16\pi, \quad \alpha_4 = \frac{15293365}{508032} + \frac{27145}{504}\nu + \frac{3085}{72}\nu^2, \\
\alpha_5 &= \pi \left(\frac{38645}{756} - \frac{65}{9}\nu \right) \left[1 + \ln \left(6^{3/2} \pi M f \right) \right], \\
\alpha_6 &= \frac{11583231236531}{4694215680} - \frac{640}{3}\pi^2 - \frac{6848}{21}\gamma + \left(-\frac{15737765635}{3048192} + \frac{2255}{12}\pi^2 \right) \nu \\
&\quad + \frac{76055}{1728}\nu^2 - \frac{127825}{1296}\nu^3 - \frac{6848}{63} \ln(64\pi M f), \\
\alpha_7 &= \pi \left(\frac{77096675}{254016} + \frac{378515}{1512}\nu - \frac{74045}{756}\nu^2 \right). \tag{6}
\end{aligned}$$

As mentioned earlier, we consider two binary systems, a $1.4 M_\odot + 10 M_\odot$ NS-BH binary and a $1.4 M_\odot + 100 M_\odot$ NS-BH binary.

B. Corrections due to modified gravity: ppE formalism

One of the most important outcomes of GW detection would be placing bounds on alternative theories of gravity [17]. Several such theories have been proposed to explain the observed late time acceleration of the Universe. Within the framework of GR the explanation is given by assuming exotic matter fields, but if classical GR is realised as a low energy limit of some more fundamental theory, we might expect non-trivial modifications to it (*e.g.* non-minimally coupled dilatons etc.).

GR has been tested with high accuracy in solar system and also through binary pulsars, and in both cases gravitational fields are weak and particles velocities are small [1]. The lack of experimental verification of GR in strong fields may not be a problem for long once we start to observe GWs directly. In particular, GW detectors in space like eLISA and DECIGO will be able to map the spacetime geometry of super-massive BHs at the center of galaxies. This can be done very accurately by observing GWs emitted by their inspiraling satellites, allowing us to test alternative theories of gravity.

For studying the modification to GR using a parameterized approach we follow the ppE formalism. The modification to the Fourier transform $H(f)$ of the GW signal (under the stationary phase approximation) from the inspiraling binary (1) would be characterized by the leading order corrections to the Fourier amplitude and the phase as

$$\mathcal{A} = \left(1 + \sum_i \alpha_i (\pi \mathcal{M} f)^{a_i} \right) A_{GR}(f), \tag{7}$$

and

$$\psi(f) = \left(\psi_{GR}(f) + \sum_i \beta_i (\pi \mathcal{M} f)^{b_i} \right). \tag{8}$$

Here $A_{GR}(f)$ is given by equation (2), and $\psi_{GR}(f)$ is given by equation (3), the standard GR expressions. The coefficients α_i and β_i , in general, may depend on parameters such as chirp mass, spin angular momentum etc. As explained in previous subsection, for the present analysis we concentrate on the modification in the phase only, meaning $A(f) = A_{GR}(f)$, i.e., $\alpha_i = 0$.

C. Noise curves

The output of a GW detector $s(t)$, can be decomposed into two components: the GW signal $h(t)$, and the detector noise $n(t)$, i.e. $s(t) = h(t) + n(t)$. For simplicity, we assume that the detector noise is stationary and Gaussian. Stationarity implies that the different Fourier components of the noise are uncorrelated, and hence the one-sided noise power spectral density (PSD) $S_n(f)$ can be defined by

$$\langle \tilde{n}(f) \tilde{n}(f') \rangle = \frac{1}{2} \delta(f - f') S_n(f),$$

where $\tilde{n}(f)$ is the Fourier transform of the noise $n(t)$. A commonly used quantity to describe sensitivity curve is square root of PSD in units of $\text{Hz}^{-1/2}$, and when integrated over positive frequencies it gives mean square amplitude of the signal in detector [18]. We describe the noise spectral densities of all the detectors used in this study below.

Future space based detectors

DECIGO: The Deci-hertz Interferometer Gravitational Wave Observatory (DECIGO) is a future plan of a space mission for observing GWs around $f \sim 0.1 - 10\text{Hz}$, proposed by [19]. The following noise curve is taken from [20]

$$S_n(f) = 6.53 \times 10^{-49} \left[1 + \left(\frac{f}{f_p} \right)^2 \right] + 4.45 \times 10^{-51} \left(\frac{f}{1\text{Hz}} \right)^{-4} \frac{1}{1 + \left(\frac{f}{f_p} \right)^2} + 4.94 \times 10^{-52} \left(\frac{f}{1\text{Hz}} \right)^{-4} \text{Hz}^{-1}, \quad (9)$$

where $f_p = 7.36\text{Hz}$.

eLISA: eLISA is a slightly down-graded mission which is derived from the Laser Interferometer Space Antenna (LISA) proposal. This mission is targeted at the low-frequency band: 0.1mHz to 1Hz . The following noise curve is taken from [21]:

$$S_n(f) = \frac{20}{4} \frac{4S_{acc}(f)/(2\pi f)^4 + S_{sn}(f) + S_{omn}(f)}{L^2} \left(1 + \frac{f}{0.41c/2L} \right)^2, \quad (10)$$

with

$$\begin{aligned} S_{acc}(f) &= 2.13 \times 10^{-29} (1 + 10^{-4}\text{Hz}/f) \text{m}^2 \text{s}^{-4} \text{Hz}^{-1}, \\ S_{sn}(f) &= 5.25 \times 10^{-23} \text{m}^2 \text{Hz}^{-1}, \\ S_{omn}(f) &= 6.28 \times 10^{-23} \text{m}^2 \text{Hz}^{-1}. \end{aligned} \quad (11)$$

where $L = 10^6\text{km}$ and c is the speed of light.

Future ground based detectors

Advanced LIGO: As the representative of the second generation of ground-based Laser Interferometer Gravitational-Wave Observatory (LIGO) The noise curve for the advanced LIGO detectors is taken from [22].

$$S_n(f) = 10^{-49} \left[\left(\frac{f}{f_0} \right)^{-4.14} - 5 \left(\frac{f}{f_0} \right)^{-2} + 111 \left(\frac{1 - \left(\frac{f}{f_0} \right)^2 + \left(\frac{f}{f_0} \right)^4 / 2}{1 + \left(\frac{f}{f_0} \right)^2 / 2} \right) \right], \quad (12)$$

where $f_0 = 215\text{Hz}$.

ET: The Einstein Telescope (ET) is a European- commission project which aims at developing the third generation Gravitational Wave observatory. The following noise curve is taken from [22]:

$$S_n(f) = 10^{-50} \left[2.39 \times 10^{-27} \left(\frac{f}{f_0} \right)^{-15.64} + 0.349 \left(\frac{f}{f_0} \right)^{-2.145} + 1.76 \left(\frac{f}{f_0} \right)^{-0.12} + 0.409 \left(\frac{f}{f_0} \right)^{1.1} \right]^2, \quad (13)$$

where $f_0 = 100\text{Hz}$. The noise curves for the various detectors are plotted in figure (1).

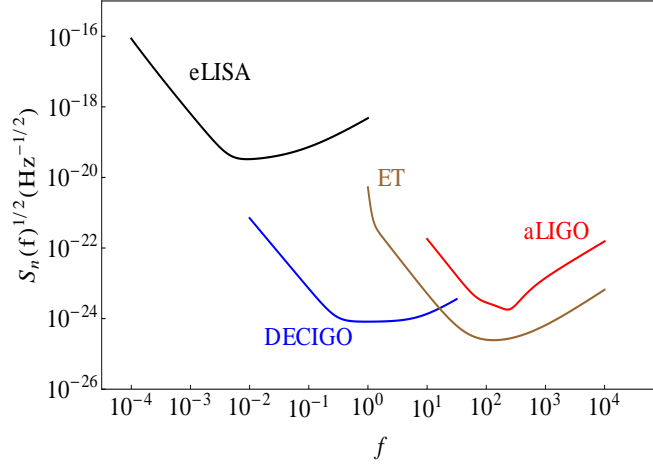


FIG. 1: Noise spectra for the different GW detectors used in this work.

D. Likelihood function and Fisher matrix

In this section we briefly overview parameter estimation and Fisher matrix method of error estimation. For a review on this topic, we refer to [23]. We assume that the GW signal depends on the parameter vector θ . In case of the PN waveform $\theta = \{\mathcal{M}, \nu, t_c, \phi_c\}$, and in case of the ppE framework $\theta = \{\mathcal{M}, \nu, t_c, \phi_c, \beta_i\}$ (in this work the ppE parameter α_i is fixed to zero for all i). Now the noise weighted inner product for two signals $h_1(t)$ and $h_2(t)$ is defined as:

$$(h_1|h_2) = 2 \int_0^\infty \frac{\tilde{h}_1^*(f)\tilde{h}_2(f) + \tilde{h}_2^*(f)\tilde{h}_1(f)}{S_n(f)} df, \quad (14)$$

where $\tilde{h}_1(f)$ and $\tilde{h}_2(f)$ are the Fourier transforms of $h_1(t)$ and $h_2(t)$, respectively, and $*$ represents the complex conjugation. The inner product is defined so that the probability that the signal depends on the parameters θ (assuming the noise is Gaussian) is given by

$$P(s|\theta) \propto e^{-(s-h(\theta)|s-h(\theta))/2}.$$

Hence, the inner product is similar to defining a chi-squared merit function. Given an output $s(t)$, the best fit GW waveform $h(\theta)$ is obtained by minimizing this inner product ([23]). For different realizations of noise, we may obtain slightly different values of the parameters, but for large signal to noise ratio they will all be centred around the correct values say $\bar{\theta}$ with some spread $\Delta\theta$. The estimation errors follow a Gaussian distribution

$$P(\Delta\theta^i) \propto e^{-\Gamma_{ij}\Delta\theta^i\Delta\theta^j/2}, \quad (15)$$

where Γ_{ij} is the Fisher matrix defined as ([15])

$$\Gamma_{ij} \equiv \left(\frac{\partial h}{\partial \theta_i} \middle| \frac{\partial h}{\partial \theta_j} \right). \quad (16)$$

The covariance matrix C is the inverse of the Fisher matrix, i.e. $C = \Gamma^{-1}$, and the root mean square error of the parameters can be evaluated from the diagonal elements as

$$\sqrt{\langle (\Delta\theta^i)^2 \rangle} = \sqrt{C^{ii}}. \quad (17)$$

When analysing the synergy effect of combining the measurements from two detectors, we take the sum of the Fisher matrices corresponding to them and then take the inverse of the matrix thus obtained:

$$\Gamma_{\text{comb}} = \Gamma_1 + \Gamma_2, \quad (18)$$

$$C_{\text{comb}} = \Gamma_{\text{comb}}^{-1}. \quad (19)$$

Studying the change in estimates by varying design sensitivity of DECIGO

We also study the synergy effect on the error estimate of various parameters by varying the sensitivities of the future space mission DECIGO (and its precursor pre-DECIGO), since its design sensitivity is still to be determined depending on the scientific gain. Here, for brevity, we simply call it DECIGO. In both better and worse directions, the sensitivities are changed by scaling the fiducial noise curve uniformly over all frequencies. Namely, the scaled DECIGO noise curves are obtained as

$$S_n(f)^{scaled} = \mathcal{K} S_n(f)^{DECIGO}, \quad (20)$$

with a constant \mathcal{K} .

III. RESULTS

In this section we explore the expected errors in the parameter estimation when we combine outputs of ground and space based detectors. We discuss results on the various parameters in the PN and the ppE waveforms for coalescing binary systems. As mentioned earlier we consider two NS-BH binary systems: a $1.4 M_{solar} + 10 M_{solar}$ binary and a $1.4 M_{solar} + 100 M_{solar}$ binary with the distance fixed at 200 Mpc. We fix the lower frequency limits at 0.1 Hz for the space based GW detectors. The space based detectors are expected to be sensitive at frequencies much below this cut off (eLISA is expected to be sensitive at as low as 0.1 mHz), but we chose this cut off since the evolution of the binary coalescence is really slow at lower frequencies. For the mass configurations we have considered in this work, it will take many years for the binaries to span the lower (10^{-5} - 0.1) frequency range and we would not be able to observe this continuously. The evolution is much faster in the mid-high frequency range and there is a chance we can observe the same events in both space and ground based detectors. For advanced-LIGO we set the lower frequency limit at 10 Hz.

A. Parameter estimation - PN expansion

Here we present the error estimates on the chirp mass, the symmetric mass ratio, and the phase and time at coalescence using the method described in the previous section. In table I and II we tabulate these errors for both independent and combined measurements. We note that there is some gain in combining space-ground measurements for all parameters. In case of the chirp mass, maximum gain is obtained for the detector pair Advanced-LIGO - eLISA, while for all the other pairs one of the GW detector completely dominates the error estimate. Similarly for the time of coalescence maximum gain is obtained for the detector pair ET-DECIGO, and for the other pairs the estimates are dominated by one of the two detectors. For the symmetric mass ratio and the phase of coalescence there is no substantial gain in combining the space-ground measurements since one of the detector always dominates the results. We further analyse the variation in the error estimates on the parameters with the variation of the DECIGO sensitivity according to equation (20). As a reference, we introduce a quantity $\Delta\theta'$ for a parameter θ , which corresponds to the error estimate from the combined measurement if that single parameter was being estimated (equation (21)). In such a case, the joint probability for the combined estimate of some parameter say θ is given by

$$\begin{aligned} P(\theta) &\propto e^{-(\Delta\theta)^2/(2(\Delta\theta_1)^2)} \times e^{-(\Delta\theta)^2/(2(\Delta\theta_2)^2)} \\ &= e^{-(\Delta\theta)^2/(2(\Delta\theta')^2)}, \end{aligned}$$

where $\Delta\theta_1$ and $\Delta\theta_2$ are the error estimates from the first and the second measurements, respectively, and

$$\Delta\theta' = \frac{\Delta\theta_1 \Delta\theta_2}{\sqrt{\Delta\theta_1^2 + \Delta\theta_2^2}}. \quad (21)$$

These reference values are, off course, different from the correct estimate $\Delta\theta(\text{combined}) = \sqrt{C_{\text{comb}}^{\theta\theta}}$ based on C_{comb} given in equation (19). The correct estimates of errors normalized by these reference values are shown in figure (2) and (3). From our study on the synergy between (scaled-)DECIGO and ET, we can infer the following about the PN template parameters: for the chirp mass, there is a wide range of sensitivities in the pre-DECIGO phase (sensitivities that are $10 - 10^7$ order of magnitude worse than DECIGO) where there is substantial gain in combining the space-ground measurements, for the symmetric mass ratio and the phase at coalescence maximum gain is obtained when the pre-DECIGO sensitivity is almost 10^2 order of magnitude worse than DECIGO, and for the time at coalescence maximum gain is achieved in the post-DECIGO phase where the sensitivity is almost an order of magnitude better than DECIGO.

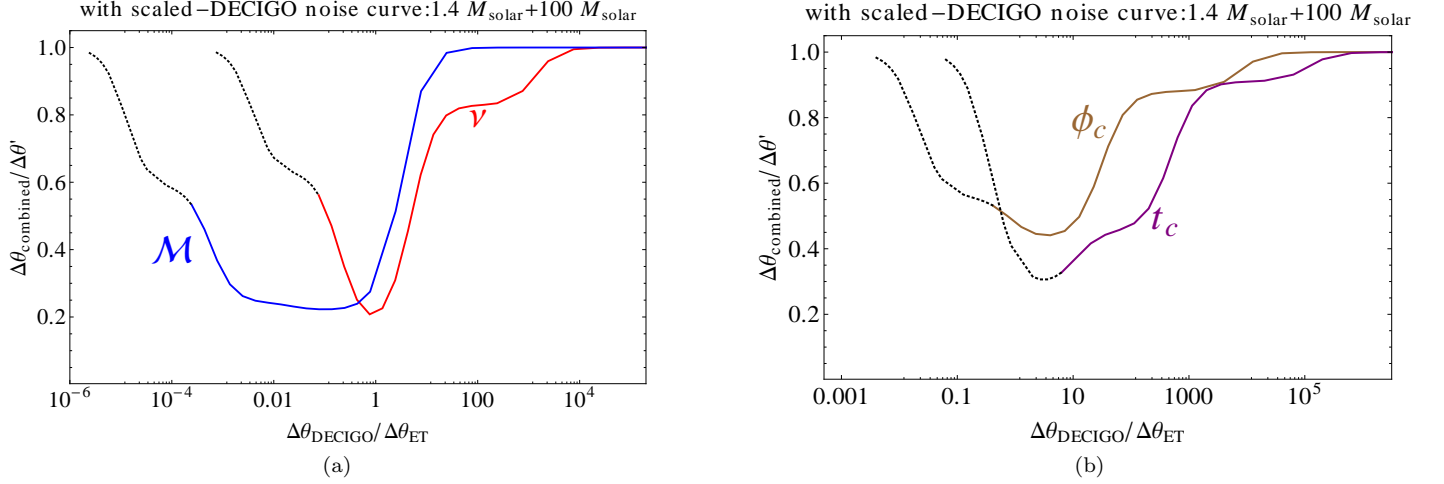


FIG. 2: Variation in the error estimates on the chirp mass and the symmetric mass ratio (a), and the time and phase at coalescence (b), obtained by varying DECIGO sensitivities. $\Delta\theta_{\text{comb}}$ ($\theta = \mathcal{M}/\nu/t_c/p_c$) is obtained as explained in section IID, and $\Delta\theta'$ is as given in equation (21). The ratio $\Delta\theta_{\text{comb}}/\Delta\theta'$ is plotted against $\Delta\theta$ as obtained from the *scaled* DECIGO measurements. The dotted curves correspond to better sensitivity than DECIGO

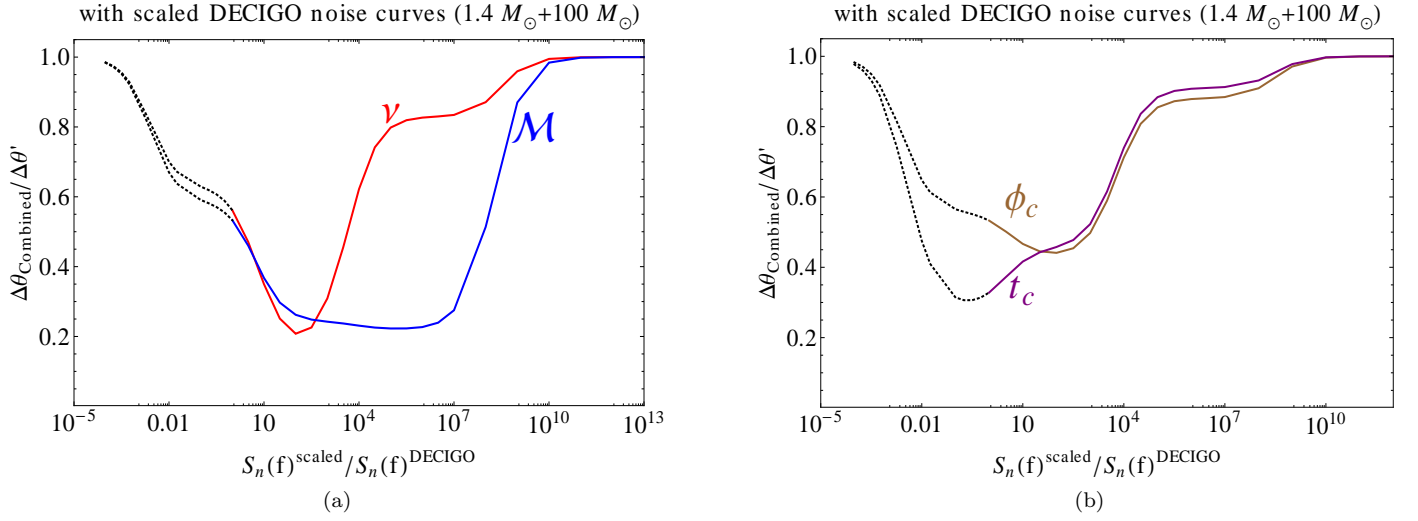


FIG. 3: Variation in the error estimates on the chirp mass and the symmetric mass ratio (a), and the time and phase at coalescence (b), with varying DECIGO sensitivities. $\Delta\theta_{\text{comb}}$ ($\theta = \mathcal{M}/\nu/t_c/p_c$) is obtained as explained in section IID, and $\Delta\theta'$ is as given in equation (21). Here too, the dotted curves correspond to better sensitivity than DECIGO.

B. ppE expansion

We present the results of the analysis for 1PN, 2PN and 3PN modifications to GR in this section. Here 1PN, 2PN and 3PN modifications mean that we fix $b = -1$, $b = -1/3$ and $b = 1/3$ in equation (8), respectively. The 1PN correction corresponds to the traditional Massive graviton theory ([11]), and the 2PN correction corresponds to Quadratic curvature theory ([11]). With distance fixed at 200 Mpc the results are shown in table III and IV for 1PN, table V and VI for 2PN and table VII and VIII for 3PN. In all cases we find some gain to the constraint on these modifications to GR when combining the measurements of the space and ground based detectors. In order to clarify the synergy effect, we present the plots similar to 2 and 3 for the parameters of the magnitude of modification

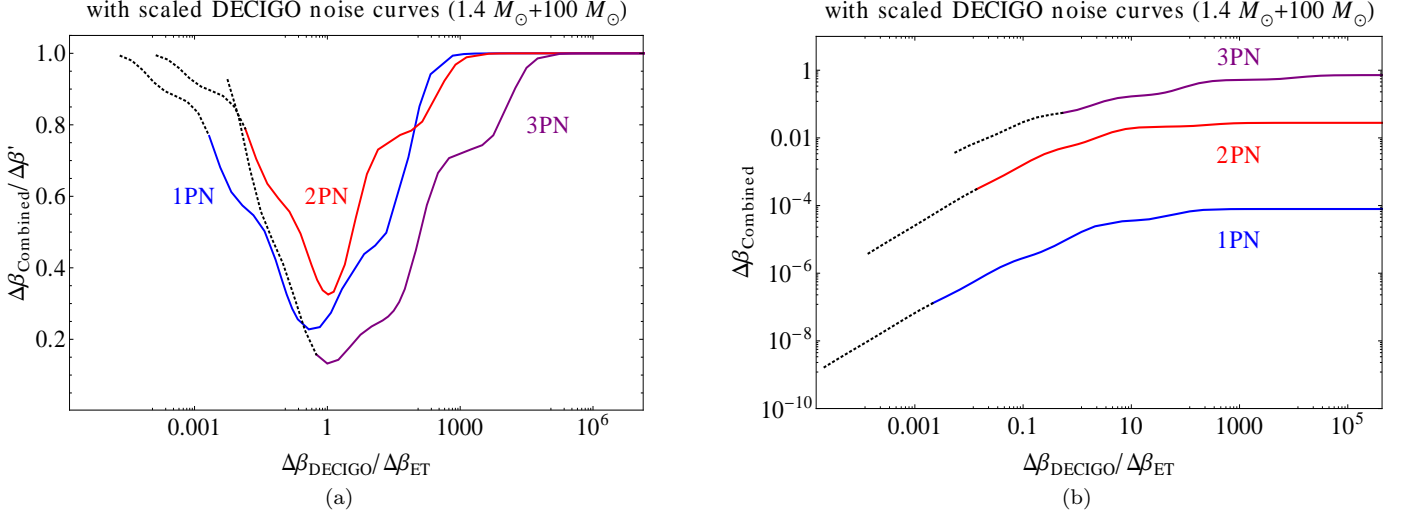


FIG. 4: Variation in the error estimates on the GR modification parameter at different PN orders. $\Delta\beta$ (combined) is obtained as explained in section II D, and $\Delta\beta'$ is as given in equation (21). The dashed part corresponds to the noise curves with better sensitivity than DECIGO

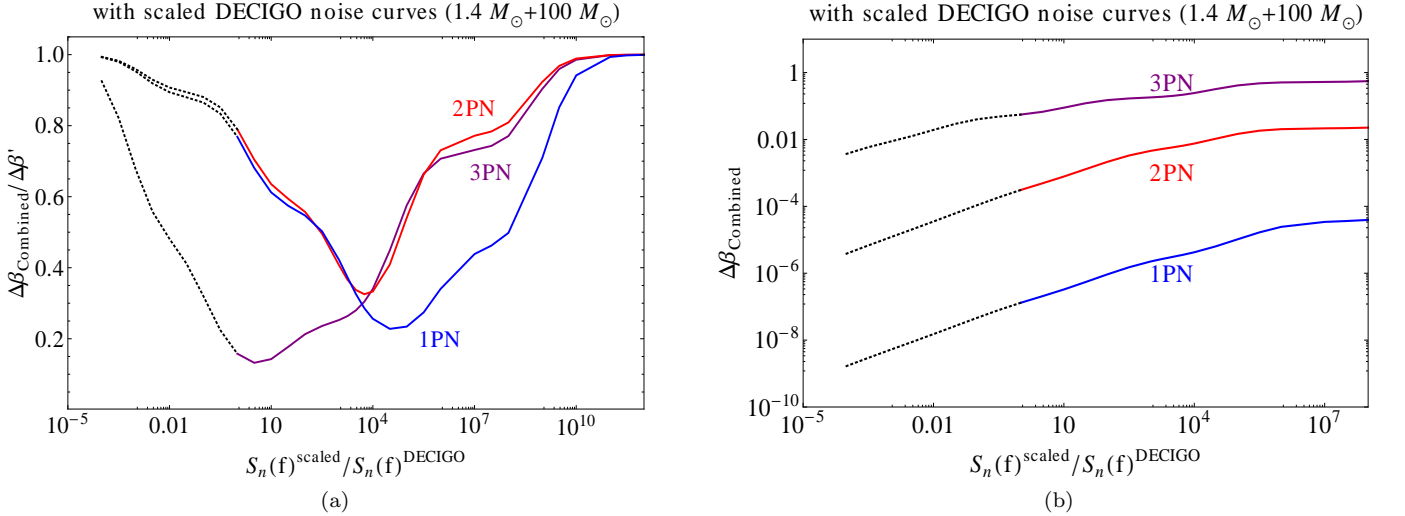


FIG. 5: Variation in the error estimates on the GR modification parameter with varying pre-DECIGO sensitivity. $\Delta\beta$ (combined) is obtained as explained in section II D, and $\Delta\beta'$ is as given in equation (21). The dotted curves correspond to better sensitivity than DECIGO.

from GR. As before, in figure (4) we plot the error estimate based on C_{comb} given in equation (19), $\Delta\beta$, relative to the reference value $\Delta\beta'$ defined by equation (21), for combined measurements from scaled-DECIGO and ET. For very low DECIGO sensitivity the error estimates are dominated by ET, while for very high DECIGO sensitivity they are dominated by DECIGO. In both limiting cases we do not have any merit of combining the space-ground measurements. However, in the middle range we have a sweet spot where the gain becomes significantly large. In this plot (figure (4)) the horizontal axis is $\Delta\beta_{\text{DECIGO}}/\Delta\beta_{\text{ET}}$. For all PN order modifications, the sweet spot appears around $\Delta\beta_{\text{DECIGO}}/\Delta\beta_{\text{ET}} = 1$, where both detectors equally contribute to constrain the parameter β . In figure (4b) we plot $\Delta\beta_{\text{Combined}}$. In the region with $\Delta\beta_{\text{DECIGO}}/\Delta\beta_{\text{ET}} \ll 1$, the error estimates are dominated by the DECIGO sensitivity, and hence they show linear dependence. In the region with $\Delta\beta_{\text{DECIGO}}/\Delta\beta_{\text{ET}} \gg 1$, the error estimates are dominated by the ET sensitivity, and hence the curves become almost flat. At around $\Delta\beta_{\text{DECIGO}}/\Delta\beta_{\text{ET}} = 1$, the slope of the curves changes. This change is not monotonic, and corresponds to the sweet spot in the figure (4a) where the true joint estimates are better than the reference estimates given by $\Delta\beta'$.

We also show these error estimates as functions of the sensitivity level of the scaled-DECIGO in figure (5). The higher order post-Newtonian terms tend to be better determined by the ground based detectors which have better sensitivities at higher frequencies. Hence, for higher PN order terms, the synergy is maximum (i.e. the space and ground detectors contribute almost equally) for higher sensitivity of scaled-DECIGO. The positions of the sweet spots in figure (3) can be understood in the same way by noticing that the leading order frequency dependences of the chirp mass, the symmetric mass ratio, and the phase and time at coalescence are 0PN, 1PN, 2.5PN and 4PN, respectively.

IV. CONCLUSIONS

In this paper we have assessed the expected synergy effects between ground and space based detectors on the parameter estimation of coalescing binary systems. Our aim is to demonstrate that the advantage of having a GW antenna which is sensitive at low frequencies, is larger than we naively expect. Larger gain in the error estimate of the GW waveform parameters is obtained when the constraints from individual ground or space detectors are almost equal. In case of the ppE parameters that characterize deviations from GR, some gain is always obtained irrespective of the level of sensitivity of the GW antenna. For lower PN order modifications some gain can be obtained even if the sensitivity of the space detector is degraded. The same argument also applies to the estimated errors in the extraction of binary parameters contained in the standard PN templates. In the present paper, neglecting the spins, we considered the chirp mass, the symmetric mass ratio, and the phase and time at coalescence, whose leading order frequency dependences on the GW phase are 0PN, 1PN, 2.5PN and 4PN, respectively. We found a sweet spot in the combined estimates of the chirp mass and the symmetric mass ratio in the pre-DECIGO phase (worse sensitivity than DECIGO). In this region, the combined error estimates are better than individual detector estimates. Substantial gain was also obtained in the joint measurement of the time and phase at coalescence. Here too the sweet spot was in the pre-DECIGO phase for the phase at coalescence, but for the time at coalescence, maximum gain was obtained with post-DECIGO sensitivity. As expected, for higher PN order parameters, synergy is obtained at higher sensitivities of the space-borne GW detector.

The sensitivity of space-borne GW antenna such as pre-DECIGO, which is the precursor mission for DECIGO, is still to be determined by considering various aspects, including the scientific gain. The study of the synergy effects reported in the present paper provides valuable information and can be taken into account to make such decisions.

Acknowledgments

This work was supported by MEXT Grant-in-Aid for Scientific Research on Innovative Areas, “New Developments in Astrophysics Through Multi-Messenger Observations of Gravitational Wave Sources”, Nos. 24103001 and 24103006. This work was also supported in part by Grant-in-Aid for Scientific Research (B) No. 26287044. R.N acknowledges support under CSIR-SRF scheme (Govt. of India), and thanks the Department of Physics, Kyoto University where part of this work was done, for hospitality. S.J acknowledges support from grant under ISRO-RESPOND program (ISRO/RES/2/384/2014-15).

-
- [1] C. M. Will, *The Confrontation between General Relativity and Experiment*, Living. Rev. Relativity., **9** 3 (2006) (cited [6 March 2015]).
 - [2] R. Narayan, J. E. McClintock, in *“General Relativity and Gravitation: A Centennial Perspective”*, Editors: A. Ashtekar, B. Berger, J. Isenberg and M.A.H. MacCallum, Cambridge University Press (2013).
 - [3] K. Yagi, *Scientific potential of DECIGO pathfinder and testing GR with space-borne gravitational wave interferometer*, Int. J. Mod. Phys. D. **22** 1 (2013).
 - [4] C. M. Will & N. Yunes, *Testing alternative theories of gravity using LISA*, Class. Quant. Grav. **21** 4367 (2004).
 - [5] N. Yunes & X. Siemens, *Gravitational-Wave Tests of General Relativity with Ground-Based Detectors and Pulsar-Timing Arrays*, Living. Rev. Relativity. **16** 9 (2013), <http://relativity.livingreviews.org/Articles/lrr-2013-9/>.
 - [6] C. M. Will, *Testing scalar-tensor gravity with gravitational-wave observations of inspiralling compact binaries*, Phys. Rev. D **50** 6058 (1994).
 - [7] E. Berti A. Buonanno & C. M. Will, *Estimating spinning binary parameters and testing alternative theories of gravity with LISA*, Phys. Rev. D **71** 084025 (2005).
 - [8] C. K. Mishra et al., *Parametrized tests of post-Newtonian theory using Advanced LIGO and Einstein Telescope*, Phys. Rev. D **82** 064010 (2010).
 - [9] K. G. Arun et al., *Probing the nonlinear structure of general relativity with black hole binaries*, Phys. Rev. D **74** 024006 (2006).

- [10] N. Yunes & F. Pretorius, *Fundamental theoretical bias in gravitational wave astrophysics and the parametrized post-Einsteinian framework*, Phys. Rev. D **80** 122003 (2009).
- [11] N. Cornish et al., *Gravitational wave tests of general relativity with the parameterized post-Einsteinian framework*, Phys. Rev. D **84** 062003 (2011).
- [12] K. Yagi and T. Tanaka, Phys. Rev. D **81** 064008 (2010).
- [13] L. Blanchet, *Gravitational Radiation from Post-Newtonian Sources and Inspiral Compact Binaries*, Living. Rev. Relativity. **17** 2 (2014), <http://relativity.livingreviews.org/Articles/lrr-2014-2/>.
- [14] B. S. Sathyaprakash & B. F. Schutz, *Physics, Astrophysics and Cosmology with Gravitational Waves*, Living. Rev. Relativity. **12** (2009) (cited [6 March 2015]).
- [15] C. Cutler & E. E. Flanagan, *Gravitational waves from merging compact binaries: How accurately can one extract the binary's parameters from the inspiral waveform?*, Phys. Rev. D **49** 6 (1994).
- [16] A. Vecchio, Phys. Rev. D **70** 042001 (2004).
- [17] K. Nordtvedt, Phys. Rev. **169** (1968) 1017; C. M. Will and K. Nordtvedt, Astrophys. J **177** (1972) 757.
- [18] C. J. Moore, R. H. Cole and C. P. L. Berry, Classical & Quantum Gravity, **32** (2015) 015014.
- [19] N. Seto, S. Kawamura & T. Nakamura, *Possibility of direct measurement of the acceleration of the Universe using 0.1-Hz band laser interferometer gravitational wave antenna in space*, Phys. Rev. Lett. **87** 221103 (2001).
- [20] K. Yagi & N. Seto, *Detector configuration of DECIGO/BBO and identification of cosmological neutron-star binaries*, Phys. Rev. D **83** 044011 (2011).
- [21] P. Amaro-Seoane et al., *Low-frequency gravitational-wave science with eLISA/NGO*, Class. Quant. Grav. **29** 124016 (2012).
- [22] D. Keppel & P. Ajith, *Constraining the mass of the graviton using coalescing black-hole binaries*, Phys. Rev. D **82** 122001 (2010).
- [23] L. S. Finn, *Detection, measurement, and gravitational radiation*, Phys. Rev. D **46** 12 (1992).

Appendix: Tabela

TABLE I: Errors estimates for PN waveform parameters for individual detector measurements. These are calculated for NS-BH binaries with masses $1.4 M_{\odot}+10 M_{\odot}$ and $1.4 M_{\odot}+100 M_{\odot}$. The distance is fixed to 200 Mpc.

Binary mass	Detector	Δt_c	$\Delta \phi_c$	$\Delta \mathcal{M}/\mathcal{M}(\%)$	$\Delta \nu/\nu(\%)$
$1.4M_{\odot}+10M_{\odot}$	DECIGO	9.16×10^{-5}	9.70×10^{-4}	9.57×10^{-8}	2.60×10^{-4}
$1.4M_{\odot}+10M_{\odot}$	eLISA	1.30×10^2	3.87×10^2	8.16×10^{-3}	2.80×10^1
$1.4M_{\odot}+10M_{\odot}$	advLIGO	3.22×10^{-4}	3.26×10^{-1}	1.62×10^{-2}	4.52×10^{-1}
$1.4M_{\odot}+10M_{\odot}$	ET	1.51×10^{-5}	1.64×10^{-2}	1.35×10^{-4}	1.31×10^{-2}
$1.4M_{\odot}+100M_{\odot}$	DECIGO	6.52×10^{-5}	2.43×10^{-3}	7.36×10^{-8}	9.36×10^{-5}
$1.4M_{\odot}+100M_{\odot}$	eLISA	1.08×10^2	2.07×10^3	6.20×10^{-2}	6.73×10^1
$1.4M_{\odot}+100M_{\odot}$	advLIGO	2.09×10^{-4}	1.49×10^{-1}	3.43×10^{-2}	3.53×10^{-2}
$1.4M_{\odot}+100M_{\odot}$	ET	1.02×10^{-5}	6.02×10^{-3}	3.00×10^{-4}	1.23×10^{-3}

TABLE II: Errors estimates for PN waveform parameters for combined detector measurements. These are calculated for NS-BH binaries with masses $1.4 M_{\odot}+10 M_{\odot}$ and $1.4 M_{\odot}+100 M_{\odot}$. The distance is fixed to 200 Mpc.

Binary mass	Detector	Δt_c	$\Delta \phi_c$	$\Delta \mathcal{M}/\mathcal{M}(\%)$	$\Delta \nu/\nu(\%)$
$1.4M_{\odot}+10M_{\odot}$	ET+DECIGO	6.04×10^{-6}	8.98×10^{-4}	9.15×10^{-8}	2.46×10^{-4}
$1.4M_{\odot}+10M_{\odot}$	ET+eLISA	1.47×10^{-5}	1.58×10^{-2}	1.03×10^{-4}	1.21×10^{-2}
$1.4M_{\odot}+10M_{\odot}$	advLIGO+DECIGO	4.95×10^{-5}	9.22×10^{-4}	9.28×10^{-8}	2.50×10^{-4}
$1.4M_{\odot}+10M_{\odot}$	advLIGO+eLISA	2.36×10^{-4}	2.55×10^{-1}	1.79×10^{-4}	2.41×10^{-1}
$1.4M_{\odot}+100M_{\odot}$	ET+DECIGO	3.31×10^{-6}	1.20×10^{-3}	3.92×10^{-8}	5.24×10^{-5}
$1.4M_{\odot}+100M_{\odot}$	ET+eLISA	9.84×10^{-6}	5.73×10^{-3}	2.28×10^{-4}	1.14×10^{-3}
$1.4M_{\odot}+100M_{\odot}$	advLIGO+DECIGO	2.56×10^{-5}	1.56×10^{-3}	4.90×10^{-8}	6.52×10^{-5}
$1.4M_{\odot}+100M_{\odot}$	advLIGO+eLISA	1.74×10^{-4}	1.36×10^{-1}	3.53×10^{-4}	2.22×10^{-2}

TABLE III: Errors estimates for ppE waveform parameters for individual detector measurements, when the modification to GR appears at the first PN order. These are calculated for NS-BH binaries with masses $1.4 M_{\odot}+100 M_{\odot}$. The distance is fixed to 200 Mpc.

Binary mass	Detector	Δt_c	$\Delta \phi_c$	$\Delta \mathcal{M}/\mathcal{M}(\%)$	$\Delta \nu/\nu(\%)$	$\Delta \beta$
$1.4M_{\odot}+10M_{\odot}$	DECIGO	1.56×10^{-4}	9.37×10^{-3}	1.85×10^{-7}	9.78×10^{-4}	2.48×10^{-7}
$1.4M_{\odot}+10M_{\odot}$	eLISA	2.59×10^2	4.91×10^3	2.98×10^{-2}	3.00×10^2	1.15×10^{-1}
$1.4M_{\odot}+10M_{\odot}$	aLIGO	7.16×10^{-4}	7.09×10^{-1}	9.13×10^{-2}	2.33	8.48×10^{-3}
$1.4M_{\odot}+10M_{\odot}$	ET	2.33×10^{-5}	1.75×10^{-2}	4.64×10^{-4}	4.44×10^{-2}	8.86×10^{-5}
$1.4M_{\odot}+100M_{\odot}$	DECIGO	7.56×10^{-5}	3.55×10^{-3}	3.76×10^{-7}	2.03×10^{-4}	1.69×10^{-7}
$1.4M_{\odot}+100M_{\odot}$	eLISA	1.22×10^2	2.12×10^3	9.18×10^{-3}	6.74×10^1	1.26×10^{-2}
$1.4M_{\odot}+100M_{\odot}$	aLIGO	7.18×10^{-4}	1.93	1.32×10^{-1}	1.16×10^{-1}	5.46×10^{-2}
$1.4M_{\odot}+100M_{\odot}$	ET	2.01×10^{-5}	3.42×10^{-2}	7.98×10^{-4}	3.36×10^{-3}	7.89×10^{-5}

TABLE IV: Errors estimates for ppE waveform parameters for combined detector measurements, when the modification to GR appears at the first PN order. These are calculated for NS-BH binaries with masses $1.4 M_{\odot}+100 M_{\odot}$. The distance is fixed to 200 Mpc.

Binary mass	Detector	Δt_c	$\Delta \phi_c$	$\Delta \mathcal{M}/\mathcal{M}(\%)$	$\Delta \nu/\nu(\%)$	$\Delta \beta$
$1.4M_{\odot}+10M_{\odot}$	ET+DECIGO	7.43×10^{-6}	4.54×10^{-3}	1.33×10^{-7}	5.84×10^{-4}	1.26×10^{-7}
$1.4M_{\odot}+10M_{\odot}$	ET+eLISA	1.91×10^{-5}	1.72×10^{-2}	1.82×10^{-4}	2.86×10^{-2}	4.50×10^{-5}
$1.4M_{\odot}+10M_{\odot}$	aLIGO+DECIGO	5.71×10^{-5}	6.12×10^{-3}	1.55×10^{-7}	7.32×10^{-4}	1.67×10^{-7}
$1.4M_{\odot}+10M_{\odot}$	aLIGO+eLISA	3.3×10^{-4}	2.60×10^{-1}	1.10×10^{-3}	6.10×10^{-1}	1.13×10^{-3}
$1.4M_{\odot}+100M_{\odot}$	ET+DECIGO	3.87×10^{-6}	1.47×10^{-3}	2.53×10^{-7}	1.09×10^{-4}	1.30×10^{-7}
$1.4M_{\odot}+100M_{\odot}$	ET+eLISA	1.59×10^{-5}	2.23×10^{-2}	3.66×10^{-4}	2.50×10^{-3}	4.72×10^{-5}
$1.4M_{\odot}+100M_{\odot}$	aLIGO+DECIGO	2.67×10^{-5}	2.15×10^{-3}	3.09×10^{-7}	1.46×10^{-4}	1.51×10^{-7}
$1.4M_{\odot}+100M_{\odot}$	aLIGO+eLISA	3.01×10^{-4}	4.95×10^{-1}	1.85×10^{-3}	5.14×10^{-2}	1.21×10^{-3}

TABLE V: Errors estimates for ppE waveform parameters for individual detector measurements, when the modification to GR appears at the second PN order. These are calculated for NS-BH binaries with masses $1.4 M_{\odot}+100 M_{\odot}$. The distance is fixed to 200 Mpc.

Binary mass	Detector	Δt_c	$\Delta \phi_c$	$\Delta \mathcal{M}/\mathcal{M}(\%)$	$\Delta \nu/\nu(\%)$	$\Delta \beta$
$1.4M_{\odot}+10M_{\odot}$	DECIGO	1.63×10^{-4}	1.27×10^{-2}	1.66×10^{-7}	5.62×10^{-4}	3.51×10^{-4}
$1.4M_{\odot}+10M_{\odot}$	eLISA	2.76×10^2	7.27×10^3	2.47×10^{-2}	1.17×10^2	1.84×10^2
$1.4M_{\odot}+10M_{\odot}$	aLIGO	3.95×10^{-3}	8.21×10^1	7.15×10^{-2}	4.21×10^1	1.60×10^1
$1.4M_{\odot}+10M_{\odot}$	ET	1.00×10^{-4}	1.90	1.21×10^{-3}	9.95×10^{-1}	3.72×10^{-1}
$1.4M_{\odot}+100M_{\odot}$	DECIGO	7.45×10^{-5}	2.53×10^{-3}	4.40×10^{-7}	3.57×10^{-4}	3.88×10^{-4}
$1.4M_{\odot}+100M_{\odot}$	eLISA	1.22×10^2	2.20×10^3	6.26×10^{-2}	6.76×10^1	2.75×10^1
$1.4M_{\odot}+100M_{\odot}$	aLIGO	1.18×10^{-3}	7.02	6.25×10^{-2}	3.19×10^{-1}	9.05×10^{-1}
$1.4M_{\odot}+100M_{\odot}$	ET	4.42×10^{-5}	2.22×10^{-1}	4.08×10^{-4}	1.14×10^{-2}	2.78×10^{-2}

TABLE VI: Errors estimates for ppE waveform parameters for combined detector measurements, when the modification to GR appears at the second PN order. These are calculated for NS-BH binaries with masses $1.4 M_{\odot}+100 M_{\odot}$. The distance is fixed to 200 Mpc.

Binary mass	Detector	Δt_c	$\Delta \phi_c$	$\Delta \mathcal{M}/\mathcal{M}(\%)$	$\Delta \nu/\nu(\%)$	$\Delta \beta$
$1.4M_{\odot}+10M_{\odot}$	ET+DECIGO	7.64×10^{-6}	5.80×10^{-3}	1.21×10^{-7}	3.76×10^{-4}	1.66×10^{-4}
$1.4M_{\odot}+10M_{\odot}$	ET+eLISA	3.27×10^{-5}	4.88×10^{-1}	2.50×10^{-4}	2.62×10^{-1}	9.65×10^{-2}
$1.4M_{\odot}+10M_{\odot}$	aLIGO+DECIGO	5.77×10^{-5}	8.09×10^{-3}	1.41×10^{-7}	4.54×10^{-4}	2.28×10^{-4}
$1.4M_{\odot}+10M_{\odot}$	aLIGO+eLISA	5.20×10^{-4}	8.23	1.83×10^{-3}	4.37	1.61
$1.4M_{\odot}+100M_{\odot}$	ET+DECIGO	4.15×10^{-6}	2.04×10^{-3}	3.13×10^{-7}	2.36×10^{-4}	3.06×10^{-4}
$1.4M_{\odot}+100M_{\odot}$	ET+eLISA	4.03×10^{-5}	1.96×10^{-1}	2.73×10^{-4}	1.03×10^{-2}	2.44×10^{-2}
$1.4M_{\odot}+100M_{\odot}$	aLIGO+DECIGO	2.67×10^{-5}	2.12×10^{-3}	3.74×10^{-7}	2.92×10^{-4}	3.52×10^{-4}
$1.4M_{\odot}+100M_{\odot}$	aLIGO+eLISA	7.57×10^{-4}	3.91	5.42×10^{-4}	1.98×10^{-1}	4.97×10^{-1}

TABLE VII: Errors estimates for ppE waveform parameters for individual detector measurements, when the modification to GR appears at the third PN order. These are calculated for NS-BH binaries with masses $1.4 M_{\odot}+100 M_{\odot}$. The distance is fixed to 200 Mpc.

Binary mass	Detector	Δt_c	$\Delta \phi_c$	$\Delta \mathcal{M}/\mathcal{M}(\%)$	$\Delta \nu/\nu(\%)$	$\Delta \beta$
$1.4M_{\odot}+10M_{\odot}$	DECIGO	2.29×10^{-4}	6.43×10^{-3}	1.29×10^{-7}	3.86×10^{-4}	2.48×10^{-1}
$1.4M_{\odot}+10M_{\odot}$	eLISA	3.98×10^2	4.68×10^3	1.65×10^{-2}	6.59×10^1	2.08×10^5
$1.4M_{\odot}+10M_{\odot}$	aLIGO	1.19×10^{-3}	7.69	2.93×10^{-2}	2.44	4.67×10^1
$1.4M_{\odot}+10M_{\odot}$	ET	4.80×10^{-5}	2.15×10^{-1}	1.52×10^{-4}	5.08×10^{-2}	1.38
$1.4M_{\odot}+100M_{\odot}$	DECIGO	1.8×10^{-4}	3.24×10^{-2}	6.83×10^{-7}	6.75×10^{-4}	4.02×10^{-1}
$1.4M_{\odot}+100M_{\odot}$	eLISA	1.38×10^2	2.50×10^3	6.51×10^{-2}	7.02×10^1	3.07×10^4
$1.4M_{\odot}+100M_{\odot}$	aLIGO	2.09×10^{-4}	2.96	7.44×10^{-2}	3.79×10^{-1}	2.97×10^1
$1.4M_{\odot}+100M_{\odot}$	ET	1.28×10^{-5}	7.81×10^{-2}	4.12×10^{-4}	7.53×10^{-3}	7.17×10^{-1}

TABLE VIII: Errors estimates for ppE waveform parameters for combined detector measurements, when the modification to GR appears at the third PN order. These are calculated for NS-BH binaries with masses $1.4 M_{\odot}+100 M_{\odot}$. The distance is fixed to 200 Mpc.

Binary mass	Detector	Δt_c	$\Delta \phi_c$	$\Delta \mathcal{M}/\mathcal{M}(\%)$	$\Delta \nu/\nu(\%)$	$\Delta \beta$
$1.4M_{\odot}+10M_{\odot}$	ET+DECIGO	1.15×10^{-5}	2.15×10^{-3}	9.73×10^{-8}	2.69×10^{-4}	6.62×10^{-2}
$1.4M_{\odot}+10M_{\odot}$	ET+eLISA	4.60×10^{-5}	1.98×10^{-1}	1.07×10^{-4}	4.53×10^{-2}	1.28
$1.4M_{\odot}+10M_{\odot}$	aLIGO+DECIGO	6.72×10^{-5}	3.70×10^{-3}	1.13×10^{-7}	3.27×10^{-4}	1.3×10^{-1}
$1.4M_{\odot}+10M_{\odot}$	aLIGO+eLISA	8.41×10^{-4}	3.99	3.85×10^{-4}	1.00	2.52×10^1
$1.4M_{\odot}+100M_{\odot}$	ET+DECIGO	7.10×10^{-6}	5.65×10^{-3}	1.30×10^{-7}	1.44×10^{-4}	5.53×10^{-2}
$1.4M_{\odot}+100M_{\odot}$	ET+eLISA	1.27×10^{-5}	6.75×10^{-2}	2.67×10^{-4}	6.2×10^{-3}	6.11×10^{-1}
$1.4M_{\odot}+100M_{\odot}$	aLIGO+DECIGO	4.31×10^{-5}	1.77×10^{-2}	3.87×10^{-7}	3.94×10^{-4}	2.00×10^{-1}
$1.4M_{\odot}+100M_{\odot}$	aLIGO+eLISA	2.03×10^{-4}	1.41	3.58×10^{-4}	1.50×10^{-1}	1.36×10^1